

VANISHING ADSORPTION ADMISSIBILITY CRITERION FOR CONTACT DISCONTINUITIES IN THE POLYMER MODEL

YULIA PETROVA, BRADLEY J. PLOHR, AND DAN MARCHESIN

ABSTRACT. We introduce the vanishing adsorption criterion for contact discontinuities and apply it to the Glimm-Isaacson model of chemical flooding of a petroleum reservoir. We prove that this criterion, which derives from a physical effect, justifies the admissibility criteria adopted previously by Keyfitz-Kranzer, Isaacson-Temple, and de Souza-Marchesin for models such that the fractional flow function depends monotonically on chemical concentration. We also demonstrate that the adsorption criterion selects the undercompressive contact discontinuities required to solve the general Riemann problem in an example model with non-monotone dependence.

1. INTRODUCTION

In this paper, we propose a new, physically-motivated admissibility criterion for contact discontinuities and analyze its relationships with existing criteria. The context for developing this admissibility criterion is the flow through porous rock of oil, water, and a chemical agent within the water, as modeled by the pair of conservation laws

$$\begin{aligned} s_t + f(s, c)_x &= 0, \\ (cs)_t + [cf(s, c)]_x &= 0. \end{aligned} \tag{1.1}$$

Here $s = s(x, t) \in [0, 1]$ is the saturation of the water phase within the oil-water fluid mixture, $c = c(x, t) \in [0, 1]$ is the concentration of the chemical agent in the water phase, and $f = f(s, c)$ is the fractional flow of water (the Buckley-Leverett flux function). Following the classical paper of Buckley-Leverett [4], we assume that $f \in C^2([0, 1]^2)$ is, for every $c \in [0, 1]$, a monotone and S-shaped function of s such that $f(0, c) = 0$, $f(1, c) = 1$, and $f_s(0, c) = f_s(1, c) = 0$, as illustrated in Fig.1.1(a).

Our main result, the equivalence of admissibility criteria (Theorem 1.5), concerns models that satisfy the following *monotonicity condition*:

$$f_c < 0 \text{ for } s \in (0, 1) \text{ and } c \in [0, 1]. \tag{1.2}$$

Such monotone behavior is typical for chemical flooding using a polymer as the chemical agent, because the viscosity of water usually increases when polymer is added. However, in Sec. 4, we consider a model that does not obey the monotonicity condition.

We focus on finding solutions of the general Riemann initial-value problem:

$$U|_{t=0} = \begin{cases} U_L & \text{for } x < 0, \\ U_R & \text{for } x > 0. \end{cases} \tag{1.3}$$

2010 *Mathematics Subject Classification.* Primary 35L65; secondary 35L67, 76L05.

Key words and phrases. Conservation law, admissibility, contact discontinuity, undercompressive, traveling waves, chemical flooding, adsorption.

(Here U denotes the state (s, c) .) The solutions we construct are scale-invariant, in that they depend on (x, t) only through the combination $\xi = x/t$. Along with smooth scale-invariant waves (centered rarefaction waves), a solution can contain centered discontinuities, which have the form

$$U(x, t) = \begin{cases} U_- & \text{if } x < \sigma t, \\ U_+ & \text{if } x > \sigma t. \end{cases} \quad (1.4)$$

A discontinuity is required to satisfy the conservation laws in the sense of distributions, which amounts to satisfying the Rankine-Hugoniot condition that constrains the left state U_- , right state U_+ , and propagation speed σ .

System (1.1) was first considered by Keyfitz and Kranzer [14] and by Isaacson [10]. It is known by various names, including the Glimm-Isaacson model, the KKIT model (referring to Keyfitz, Kranzer, Isaacson, and Temple), and the chemical flooding model. It is closely related to several models of multi-phase flow in porous media, including chromatography [19], gas flooding [18], CO₂-flooding [23], and other examples described in books on enhanced oil recovery [2, 15, 3]. We shall call it the polymer model.

The system (1.1) has the following two characteristic speeds (see, *e.g.*, Temple [22]):

- The saturation (or s -type) characteristic speed is $\lambda^s = f_s$, which has associated right eigenvector $r^s = (1, 0)^T$; it is genuinely nonlinear except where $f_{ss} = 0$. For an s -type solution of system (1.1), c has a fixed value and s is governed by the first equation in system (1.1), which is the Buckley-Leverett scalar conservation law. Such a solution can be an s -rarefaction wave, an s -shock wave, or a contiguous group of such waves, which we call an s -wave group.
- The concentration (or c -type) characteristic speed is $\lambda^c = f/s$, which is linearly degenerate (meaning that $(D\lambda^c)r^c \equiv 0$, where r^c is a corresponding right eigenvector field). As a consequence, its rarefaction curves and Hugoniot loci coincide and every c -type solution is a contact discontinuity, *i.e.*, a weak solution (1.4) such that

$$\lambda^c(U_-) = \sigma = \lambda^c(U_+), \quad (1.5)$$

which we call a c -wave.

A challenging feature of system (1.1) is its loss of strict hyperbolicity in the interior of state space: the coincidence locus, where the characteristic speeds coincide, comprises not only the boundary line $s = 0$ but also the set

$$\mathcal{C} := \{U : \lambda^s(U) = \lambda^c(U) \text{ and } s \neq 0\}, \quad (1.6)$$

which we call the interior coincidence locus. This set is a smooth curve along which s is parametrized by c , as illustrated in Fig. 1.1(b). To the left and right of the interior coincidence locus are the separate regions of strict hyperbolicity

$$\begin{aligned} \{\lambda^s > \lambda^c\} &:= \{U : \lambda^s(U) > \lambda^c(U)\}, \\ \{\lambda^s < \lambda^c\} &:= \{U : \lambda^s(U) < \lambda^c(U)\}. \end{aligned}$$

Relative to more complete models of fluid flow, the conservation laws (1.1) have been simplified by neglecting some physical effects. To account for these effects, the conservation laws must be supplemented by an admissibility criterion that selects the discontinuities that appear in a Riemann solution, just as the conservation laws governing gas dynamics is amended by an entropy condition [16].

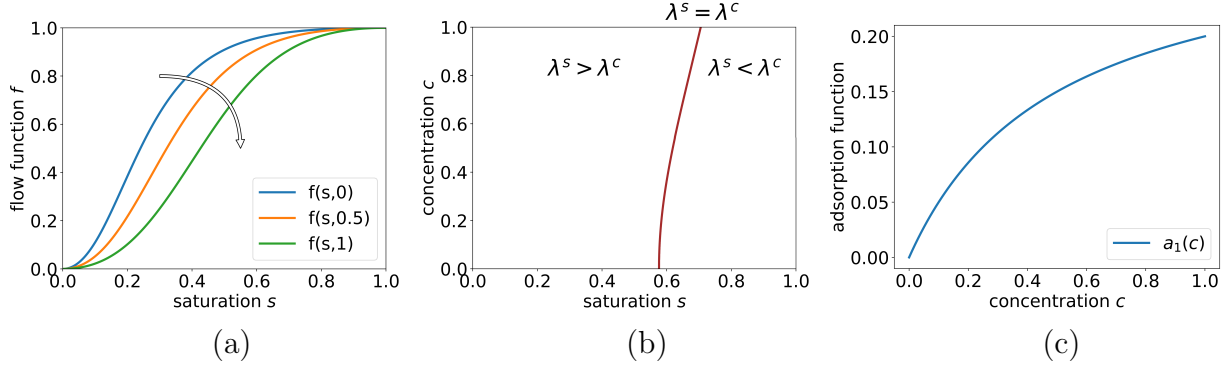


FIGURE 1.1. (a) The fractional flow function $f(s, c)$ for the monotone polymer model, plotted *vs.* s for some fixed values of c . (b) The (s, c) -space, divided by the interior coincidence curve \mathcal{C} into two regions of strict hyperbolicity, $\{\lambda^s > \lambda^c\}$ and $\{\lambda^s < \lambda^c\}$. (c) The adsorption function $a_1(c)$, which appears in Eq. (1.9) below.

Each s -wave group solves the Buckley-Leverett scalar conservation law for a fixed value of c , so we require it to satisfy the standard Oleřnik admissibility criterion [17]. In contrast, a c -wave is a contact discontinuity, for which there is no standard admissibility criterion. In gas dynamics, the archetype of conservation laws, every contact discontinuity is admissible, but blanket admissibility of contact discontinuities does not carry over to all systems. The vanishing viscosity admissibility criterion [7] does not apply to contact discontinuities, which lack nonlinear wave focusing to balance viscous spreading, so that traveling waves are not supported.

Keyfitz and Kranzer [14] and Isaacson [10] recognized that, for system (1.1), treating all contact discontinuities as admissible leads to nonuniqueness of solutions of Riemann problems. Instead, they both adopted the following admissibility criterion for contact discontinuities, calling it the generalized Lax entropy condition, and deduced the existence and uniqueness of solutions of the general Riemann problem (1.3) for system (1.1).

Definition 1.1 (Criterion of Keyfitz and Kranzer [14] and of Isaacson [10]). A c -wave, *i.e.*, a contact discontinuity, is admissible if one of the following conditions holds:

$$\text{either } \sigma < \lambda^s(U_-) \text{ and } \sigma < \lambda^s(U_+); \quad (1.7)$$

$$\text{or } \sigma > \lambda^s(U_-) \text{ and } \sigma > \lambda^s(U_+). \quad (1.8)$$

In addition, a c -wave is deemed admissible if it is the limit of a sequence of c -waves satisfying (1.7) or a sequence satisfying (1.8).

Isaacson and Temple [11] used an equivalent reformulation of this admissibility criterion.

Definition 1.2 (Criterion of Isaacson and Temple [11]). A c -wave is admissible if either (1) both U_- and U_+ belong to $\{\lambda^s \geq \lambda^c\}$ or (2) both U_- and U_+ belong to $\{\lambda^s \leq \lambda^c\}$.

A generalization of these criteria was proposed by de Souza and Marchesin [6], who named it the KKIT criterion.

Definition 1.3 (Criterion of de Souza and Marchesin [6]). A c -wave is admissible if c varies continuously and monotonically along a sequence of contact curves leading from U_- to U_+ .

In this paper, we show that the foregoing admissibility criteria result from a physical phenomenon, namely adsorption of the chemical agent onto the surface of the porous rock, in the limit when the adsorption coefficient tends to zero. In particular, we consider the following pair of conservation laws (first analyzed by Johansen and Winther [13]):

$$\begin{aligned} s_t + f(s, c)_x &= 0, \\ [c s + \alpha a_1(c)]_t + [c f(s, c)]_x &= 0, \end{aligned} \tag{1.9}$$

supplemented by a vanishing viscosity admissibility criterion. This system is distinguished from system (1.1) by the term $\alpha a_1(c)$, which is the equilibrium amount of chemical agent adsorbed onto the rock surface when the concentration is c . Here $\alpha > 0$ and the smooth function $a_1(c)$ is assumed to be strictly increasing ($a_1' > 0$) and strictly concave ($a_1'' < 0$), as depicted in Fig.1.1(c). We will refer to system (1.9) as model M_α . In particular, system (1.1) is model M_0 .

Although adsorption of a chemical agent onto a porous rock is commonplace, the adsorption term $\alpha a_1(c)$ is usually small compared to $c s$. Often, the effect of adsorption is expected to be negligible and α is set to zero. However, as we shall see, even small, but nonzero, adsorption serves to distinguish the admissible contact discontinuities. Thus motivated, we propose the following admissibility criterion.

Definition 1.4 (Vanishing adsorption admissibility criterion for contact discontinuities). A contact discontinuity for system (1.1) is admissible provided that it is the L^1_{loc} limit, as $\alpha \rightarrow 0^+$, of a sequence of admissible solutions of the Riemann problem (1.3) for system (1.9).

Remark 1.1. *We emphasize that a contact discontinuity is admissible according to Def. 1.4 not only if it is a limit of shock waves but also if it is a limit of rarefaction waves, composite waves, or more general Riemann solutions for system (1.9). (In contrast, for the vanishing viscosity admissibility criterion, a shock wave must be the limit of traveling wave solutions.)*

Consider a polymer model (1.1) that satisfies the monotonicity condition (1.2). As observed in Refs. [11, 6], the set of admissible Riemann solutions is the same under each of the following criteria for contact discontinuities:

- Keyfitz-Kranzer/Isaacson criterion of Def. 1.1;
- Isaacson-Temple criterion of Def. 1.2;
- de Souza-Marchesin criterion of Def. 1.3.

The main result of this paper is the following equivalence of admissibility criteria:

Theorem 1.5. *For a polymer model (1.1) that satisfies the monotonicity condition (1.2), the set of admissible Riemann solutions under the vanishing adsorption criterion of Def. 1.4 is the same as under the criteria of Defs. 1.1-1.3.*

As a consequence of the equivalence of admissibility criteria, Isaacson's proof of existence and uniqueness [10] yields the following corollary:

Corollary 1.6. *For a model (1.1) that conforms to the monotonicity condition (1.2), if the vanishing adsorption admissibility criterion for contact discontinuities is adopted, then the solution of the general Riemann problem (1.3) exists and is unique.*

Remark 1.2. *We emphasize that Theorem 1.5 applies to the specific model (1.1) with monotone variation of f in c . We will see that this equivalence of criteria does not hold for non-monotone models.*

Contact discontinuities obeying the Keyfitz-Kranzer/Isaacson inequalities (1.7) and (1.8) are not the only ones that occur in Riemann solutions. In Ref. [6], de Souza and Marchesin made use of contact discontinuities that satisfy

$$\lambda^s(U_-) < \sigma < \lambda^s(U_+) \quad (1.10)$$

along with their admissibility criterion of Def. 1.3. They showed that these discontinuities (which they called transitional contact discontinuities) are needed to solve certain Riemann problems.

These discontinuities are analogues, for the case of a linearly degenerate characteristic family, of non-classical shock waves that occur in various systems of conservation laws. Adopting the terminology used for such waves to the present context, we say that a contact discontinuity has a *crossing* configuration of characteristic paths [9] if inequalities (1.10) hold, and we will call it *undercompressive* [20] if, in addition, it is admissible in an appropriate sense.

Example 1.7. An example [1] of a polymer model (1.1), presented in Sec. 4, has a contact discontinuity with a crossing configuration of characteristics that satisfies the de Souza-Marchesin criterion but neither the Keyfitz-Kranzer/Isaacson nor the Isaacson-Temple criteria. (Necessarily, the monotonicity condition (1.2) does not hold for this model.) Therefore, the set of admissible Riemann solutions is different for these different criteria.

In Sec. 4, we demonstrate the adsorption admissibility of undercompressive contacts for a particular non-monotone polymer model:

Theorem 1.8. *The undercompressive contact discontinuities found by de Souza and Marchesin [6] satisfy the vanishing adsorption admissibility criterion.*

The paper is organised as follows. In Sec. 2, we present some background on conservation laws and review properties of the chemical flooding models (1.1) and (1.9). In Sec. 3, we prove the equivalence of admissibility criteria (Theorem 1.5). Finally, in Sec. 4, we describe Example 1.7 and prove that undercompressive contact discontinuities obey the adsorption admissibility criterion (Theorem 1.8).

2. BACKGROUND ON CONSERVATION LAWS AND POLYMER FLOODING MODELS

In this section, we recall important properties of hyperbolic conservation laws in general and of the polymer models M_α with $\alpha \geq 0$ in particular. More details can be found in textbooks, such as Refs. [21, 5], in previous work [14, 10, 12, 6] on the polymer model without adsorption, and in Ref. [13] for the polymer model with adsorption.

2.1. Basic notions for hyperbolic conservation laws. Systems (1.1) and (1.9) take the form of a conservation law

$$G(U)_t + F(U)_x = 0 \quad (2.1)$$

governing the evolution of the state $U \in \Omega \subseteq \mathbb{R}^2$. Here $G(U)$ is a vector of conserved quantities and $F(U)$ is a vector of flux functions. We intend to solve the Riemann initial-value problem (1.3). Because the governing equations and initial data are scale-invariant, we seek scale-invariant solutions, meaning that U depends on (x, t) solely through $\xi := x/t$.

2.1.1. *Rarefaction waves.* In a space-time region where U is continuously differentiable, system (2.1) requires that

$$DG(U) U_t + DF(U) U_x = 0. \quad (2.2)$$

When U is scale invariant, this equation reduces to the ordinary differential equation

$$[-\xi DG(U) + DF(U)] U_\xi = 0. \quad (2.3)$$

We distinguish two kinds of solutions of this equation.

- A constant state: in an open interval of ξ , $U \equiv U^{\text{const}}$ is constant, so that $U_\xi \equiv 0$.
- A rarefaction wave: in an open interval of ξ , U_ξ is a right eigenvector of the characteristic matrix

$$A(U) := [DG(U)]^{-1} DF(U), \quad (2.4)$$

and ξ equals the corresponding eigenvalue $\lambda(U)$, which is called a characteristic speed.

State space can be decomposed into three parts. The strictly hyperbolic region is the set of states U such that $A(U)$ has two distinct real eigenvalues. In a sufficiently small neighborhood of a state in this region, each eigenvalue is a smooth function $\lambda(U)$, and a corresponding smooth right eigenvector field $r(U)$ can be constructed. In contrast, in the elliptic region, the two eigenvalues of $A(U)$ are not real, so that the null space of the matrix in brackets in Eq. (2.3) is empty. Finally, on the coincidence locus, the matrix $A(U)$ has a repeated eigenvalue, *i.e.*, its discriminant is zero.

Starting from state U_- in the strictly hyperbolic region, a rarefaction wave can be constructed for the characteristic speed $\lambda(U)$ by (i) solving the initial-value problem $U_\eta = r(U)$ with $U(0) = U_-$, (ii) inverting the relationship $\lambda(U(\eta)) = \xi$, and (iii) replacing the parameter η by ξ in $U(\eta)$ to obtain $U^{\text{raref}}(\xi)$. Step (ii) requires $U(\eta)$ to lie entirely within a connected component of the region of state space where $(D\lambda)r \neq 0$. Therefore the subset of state space where $(D\lambda)r = 0$ plays an important role when constructing rarefaction waves associated to $\lambda(U)$. Two situations are typical: either this subset is a curve, called the inflection locus for $\lambda(U)$; or $(D\lambda)r \equiv 0$ throughout an open region in which $\lambda(U)$ is said to be linearly degenerate.

2.1.2. *Shock waves.* A shock wave is a scale-invariant discontinuous solution of system (2.1). Such a solution, which takes the form (1.4), separates left and right states U_- and U_+ and propagates with speed σ . The weak form of the conservation law (2.1) requires that the Rankine-Hugoniot condition

$$-\sigma [G(U_+) - G(U_-)] + F(U_+) - F(U_-) = 0 \quad (2.5)$$

holds.

The Hugoniot locus $\mathcal{H}(U_-)$ for reference state U_- consists of all states U_+ such that there exists a speed σ for which the Rankine-Hugoniot condition (2.5) is satisfied. Usually, the Hugoniot locus for U_- is a smooth curve except at U_- , where it crosses itself.

2.2. Polymer models, with and without adsorption.

2.2.1. *Characteristic speeds.* For the system (1.9), the characteristic matrix (2.4) is

$$A = \begin{pmatrix} f_s & f_c \\ 0 & f/(s + \alpha a'_1) \end{pmatrix}. \quad (2.6)$$

The eigenvalues of A , *i.e.*, the characteristic speeds for the system, are

$$\lambda^s = f_s \quad \text{and} \quad \lambda_\alpha^c := f/(s + \alpha a'_1). \quad (2.7)$$

We choose the right eigenvectors corresponding to λ^s and λ_α^c to be

$$r^s := \begin{pmatrix} 1 \\ 0 \end{pmatrix} \quad \text{and} \quad r_\alpha^c := \begin{pmatrix} -f_c \\ \lambda^s - \lambda_\alpha^c \end{pmatrix}. \quad (2.8)$$

As both characteristic speeds are real, this model is hyperbolic. However, the characteristic speeds coincide, not only on the boundary line $s = 0$, but also on the set

$$\mathcal{C}_\alpha := \{U : \lambda^s(U) = \lambda_\alpha^c(U) \text{ and } s \neq 0\}, \quad (2.9)$$

which generalizes the interior coincidence locus (1.6). As is easily seen by graphing f vs. s with c fixed, \mathcal{C}_α is a smooth curve along which s is parametrized by c , which we write as $s = s_{\text{coinc}}(c)$.

2.2.2. Rarefaction waves. For a rarefaction wave associated to the s -type characteristic speed, the formula for r^s entails that c remains constant. Thus it is a solution of the Buckley-Leverett scalar conservation law (the first of Eqs. (1.1)) for fixed c . Such a solution cannot cross the s -type inflection locus, which is the curve in the (s, c) -plane where $f_{ss} = 0$.

The c -type characteristic speed is genuinely nonlinear except where the following quantity vanishes:

$$(D\lambda_\alpha^c) r_\alpha^c = -\alpha \frac{f a_1''(\lambda^s - \lambda_\alpha^c)}{(s + \alpha a_1')^2}. \quad (2.10)$$

When $\alpha = 0$, it vanishes identically, *i.e.*, the c -type speed is linearly degenerate: $\lambda_0^c(U)$ remains constant along each integral curve of the ordinary differential equation $\dot{U} = r_0^c(U)$. We denote the integral curve containing U_- , which is the level curve $\lambda_0^c(U) = \lambda_0^c(U_-)$, by $\mathcal{I}_0(U_-)$; such curves foliate state space. These curves cannot be used to construct c -type rarefaction waves; rather, they are loci of contact discontinuities.

When $\alpha > 0$, the vanishing of expression (2.10) defines the c -type inflection locus, which accordingly is the union of the interior coincidence locus \mathcal{C}_α with the boundary line $s = 0$ (because $f = 0$ only if $s = 0$). The c -type integral curve $\mathcal{I}_\alpha(U_-)$ through a state U_- is the solution of the ordinary differential equation

$$U_\eta = r_\alpha^c(U) \quad (2.11)$$

that emanates from U_- at $\eta = 0$ in both directions, *i.e.*, for negative as well as positive η . A c -type rarefaction wave is constructed, as previously described, from any segment within an integral curve that does not cross the inflection locus (meaning, in practice, the interior coincidence locus).

Remark 2.1. *By virtue of the monotonicity assumption (1.2), $\mathcal{I}_\alpha(U_-)$ can be constructed by solving the ordinary differential equation*

$$\frac{dc}{ds} = \frac{\lambda^s - \lambda_\alpha^c}{-f_c} \quad (2.12)$$

to find c as a function of s . Thus $\mathcal{I}_\alpha(U_-)$ takes the form of an arch with horizontal tangent at the interior coincidence locus, as illustrated in Fig. 2.1. Because the right-hand side of Eq. (2.12) is smooth in α as well as (s, c) , $\mathcal{I}_\alpha(U_-)$ varies smoothly in α , and it approaches $\mathcal{I}_0(U_-)$ as $\alpha \rightarrow 0^+$.

2.2.3. *Shock waves.* For system (1.9), the Rankine-Hugoniot condition (2.5) for states $U_- = (s_-, c_-)$ and $U_+ = (s_+, c_+)$ is the pair of equations

$$-\sigma \Delta s + \Delta f = 0, \quad (2.13)$$

$$-\sigma [\bar{s} \Delta c + \alpha \Delta a_1] + \bar{f} \Delta c + [-\sigma \Delta s + \Delta f] \bar{c} = 0. \quad (2.14)$$

The notation used here is $\Delta J := J_+ - J_-$ and $\bar{J} := (J_- + J_+)/2$, and we have invoked the identity $\Delta(JK) = (\Delta J)\bar{K} + \bar{J}\Delta K$.

Let us define the smooth function

$$\langle a'_1 \rangle := \int_0^1 a'_1((1-\theta)c_- + \theta c_+) d\theta \quad (2.15)$$

of c_- and c_+ , which satisfies $\Delta a_1 = \langle a'_1 \rangle \Delta c$. Using this identity and the first Rankine-Hugoniot equation, the second one becomes

$$\{-\sigma [\bar{s} + \alpha \langle a'_1 \rangle] + \bar{f}\} \Delta c = 0. \quad (2.16)$$

We conclude that either $c_+ = c_-$ or the quantity in braces vanishes. In the former case, the first Rankine-Hugoniot equation is the jump condition of the Buckley-Leverett scalar conservation law for a fixed value of c . In the latter case, adding and subtracting $1/2$ times the first equation to the vanishing of the braces gives the equivalent pair of equations

$$-\sigma [s_{\pm} + \alpha \langle a'_1 \rangle] + f(s_{\pm}, c_{\pm}) = 0. \quad (2.17)$$

Recalling our assumptions that $\alpha \geq 0$ and $a'_1 > 0$, we observe that the quantity in brackets is positive when $s_{\pm} > 0$.

Therefore, the Rankine-Hugoniot condition has two types of solutions:

- a saturation (or s -type) discontinuity, for which $c_+ = c_- =: c$ and

$$-\sigma (s_+ - s_-) + f(s_+, c) - f(s_-, c) = 0; \quad (2.18)$$

- a concentration (or c -type) discontinuity, which satisfies

$$\frac{f(s_+, c_+)}{s_+ + \alpha \langle a'_1 \rangle} = \sigma = \frac{f(s_-, c_-)}{s_- + \alpha \langle a'_1 \rangle}. \quad (2.19)$$

The branches of the Hugoniot locus of a state U_- comprising s -type and c -type discontinuities are denoted $\mathcal{H}_\alpha^s(U_-)$ and $\mathcal{H}_\alpha^c(U_-)$, respectively.

Remark 2.2. When $\alpha = 0$, a c -type discontinuity is a contact discontinuity (1.5), so that $\mathcal{H}_0^c(U_-)$ coincides with the integral curve $\mathcal{I}_0(U_-)$. When $\alpha > 0$, $\mathcal{H}_\alpha^c(U_-)$ is the zero-set of

$$\mathcal{F} := f(s_+, c_+)/[s_+ + \alpha \langle a'_1 \rangle] - f(s_-, c_-)/[s_- + \alpha \langle a'_1 \rangle],$$

which is a smooth function of α as well as (s_+, c_+) . Moreover, when evaluated at $\alpha = 0$, the derivative \mathcal{F}_{c_+} equals $f_c(s_+, c_+)/s_+$, which is nonzero for all $s_+ > 0$. Hence the zero-set is a smooth curve, with c parametrized by s , so long as $\alpha > 0$ is sufficiently small. Thus $\mathcal{H}_\alpha^c(U_-)$ varies smoothly with α and approaches $\mathcal{H}_0^c(U_-)$ as $\alpha \rightarrow 0^+$. Also, for each c_+ , $\mathcal{F}_{s_+} = [f_s(s_+, c_+) - \sigma]/[s_+ + \alpha \langle a'_1 \rangle]$ vanishes at a unique value of s_+ (which exceeds $s_{\text{coinc}}(c_+)$ because $a''_1 < 0$), so that $\mathcal{H}_\alpha^c(U_-)$ takes the form of an arch with horizontal tangent near to the interior coincidence locus.

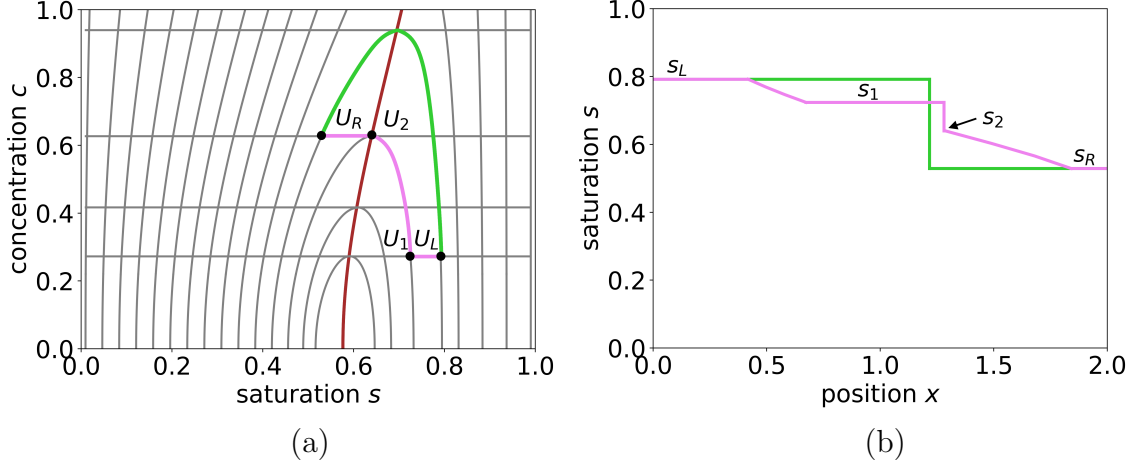


FIGURE 2.1. (a) Horizontal lines are s -type branches of Hugoniot loci, and arches are c -type branches. The brown curve is the interior coincidence locus. The violet and green curves on both (a) and (b) represent two possible solutions of a particular Riemann problem, which exemplify multiplicity of solutions in the absence of an admissibility condition for contact discontinuities.

2.2.4. *Admissibility.* A solution of a Riemann problem is an assembly of s -wave groups, c -waves, and constant states ordered by speed. We shall use the notation $U \xrightarrow{s} U'$ (respectively, $U \xrightarrow{c} U'$) to denote an s -wave group (resp., a c -wave) leading, in the direction of increasing speed, from a state U to another state U' .

As is well-known for the Buckley-Leverett conservation law, an s -wave group can be a rarefaction wave, a shock wave, or a composite wave (*i.e.*, a sonic shock wave adjoining a rarefaction fan). An s -wave group is required to satisfy the Oleĭnik admissibility criterion [17]; equivalently, each s -type shock wave in the solution must satisfy the vanishing viscosity criterion [7].

Likewise, if $\alpha > 0$, the vanishing-viscosity admissibility criterion can be applied to c -type shock waves [13]. In contrast, when $\alpha = 0$, the admissibility of a c -wave (*i.e.*, a contact discontinuity) does not have a foundation based on a physical phenomenon. Resolving this issue is the main purpose of this paper.

2.2.5. *Nonuniqueness of Riemann solutions.* Unless we impose some admissibility criterion on c -waves in model M_0 , Riemann problems can have multiple solutions, as illustrated by the following example depicted in Fig. 2.1. Take two points $U_L = (s_L, c_L) \in \{\lambda^s < \lambda^c\}$ and $U_R = (s_R, c_R) \in \{\lambda^s > \lambda^c\}$ that lie on the same contact curve but are on opposite sides of the interior coincidence locus. There exist at least two solutions to the Riemann problem:

$$U_L \xrightarrow{c} U_R \quad \text{and} \quad U_L \xrightarrow{s} U_1 \xrightarrow{c} U_2 \xrightarrow{s} U_R.$$

(In fact, there are infinitely many solutions.) Here $U_2 = (s_2, c_R)$ is a point on \mathcal{C}_0 and $U_1 = (s_1, c_L) \in \{\lambda^s < \lambda^c\}$ is the unique point on the same contact curve as U_2 with concentration c_L .

2.2.6. *Layout of solutions to Riemann problems.* The types of waves that appear in a Riemann solution, as well as their relative speeds, depend on the locations of both U_L and

U_R with respect to certain curves. Let us recount how solutions of the general Riemann problem (1.3) are laid out in the (s, c) -plane.

In Figs. 2.2 and 2.3 we present the Riemann solutions when (a) $U_L \in \{\lambda^s > \lambda^c\}$ and (b) $U_L \in \{\lambda^s < \lambda^c\}$. (If U_L lies on the interior coincidence locus, Riemann solutions can be obtained by taking appropriate limits of solutions in these cases.) Figures 2.2(a) and (b) are for the polymer model without adsorption ($\alpha = 0$), whereas Figs. 2.3(a) and (b) correspond to the model with adsorption ($\alpha > 0$).

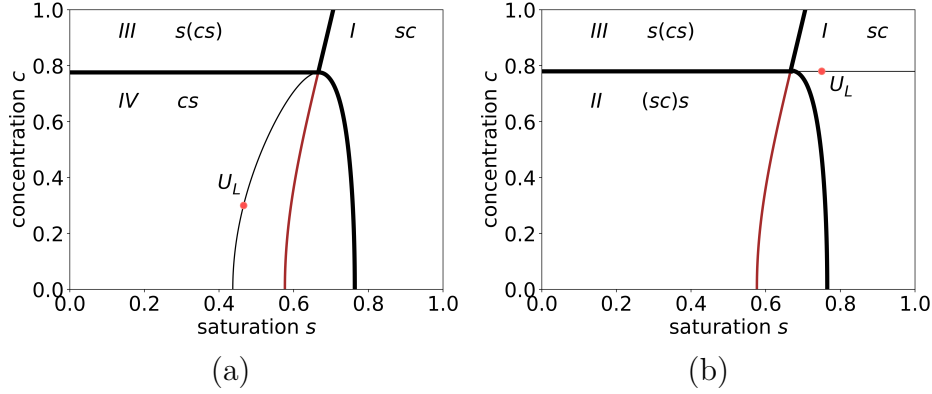


FIGURE 2.2. Polymer model M_0 : decomposition into U_R -regions I, II, *etc.*, along with the solution structure, depending on the location of the left state U_L : (a) $U_L \in \{\lambda^s > \lambda^c\}$; (b) $U_L \in \{\lambda^s < \lambda^c\}$.

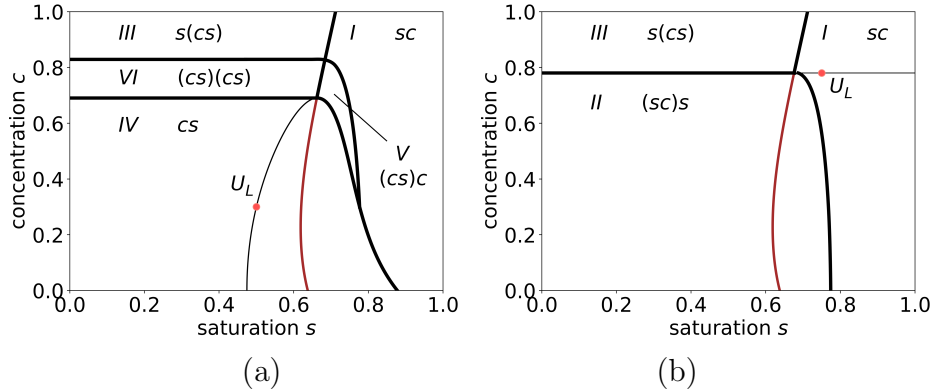


FIGURE 2.3. Polymer model M_α with $\alpha > 0$: decomposition into U_R -regions I, II, *etc.*, along with the solution structure, depending on the location of the left state U_L : (a) $U_L \in \{\lambda^s > \lambda^c\}$; (b) $U_L \in \{\lambda^s < \lambda^c\}$.

Let us illustrate how to interpret these diagrams by explaining Fig. 2.2(b) for M_0 in more detail. For a fixed left state $U_L \in \{\lambda^s < \lambda^c\}$, there are three different sequences of waves that appear in Riemann solutions, depending on the location of the right state U_R :

- U_R in region I: the solution is $U_L \xrightarrow{s} U_M \xrightarrow{c} U_R$;
- U_R in region II: the solution is $U_L \xrightarrow{s} U_1 \xrightarrow{c} U_M \xrightarrow{s} U_R$, where the s -wave group leads from U_L to the unique state $U_1 = (s_1, c_L) \in \mathcal{C}_0$ and the adjoining contact discontinuity leads from U_1 to the unique state $U_M = (s_2, c_R) \in \{\lambda^s > \lambda^c\} \cap \mathcal{H}_0^c(U_1)$;

- U_R in region III: the solution is $U_L \xrightarrow{s} U_M \xrightarrow{c} U_2 \xrightarrow{s} U_R$, where the s -wave group leading to U_R begins at the unique state $U_2 = (s_2, c_R) \in \mathcal{C}_0$ and the adjoining contact leading to U_2 begins at the unique state $U_M = (s_1, c_L) \in \{\lambda^s < \lambda^c\} \cap \mathcal{H}_0^c(U_2)$.

The boundary between regions I and III is the part of the interior coincidence locus \mathcal{C}_0 with $c \geq c_L$, whereas regions II and III are separated by the horizontal line $c = c_L$ in $\{\lambda^s > \lambda^c\}$ and the boundary between regions I and II is the part of the contact curve containing the state $U_0 = (s, c_L) \in \mathcal{C}_0$ that lies within $\{\lambda^s < \lambda^c\}$.

Figure 2.2(a) for $\alpha = 0$ and Figs. 2.3(a) and (b) for $\alpha > 0$ are interpreted in a similar fashion. See Ref. [13] for details.

Another way of representing these three solutions is to draw graphs of the functions $s(x/t)$ and $c(x/t)$ for fixed time $t > 0$. These graphs appear in Figs. 2.4 (1a), (1b), and (1c). In addition, Figs. 2.4 (2a)-(2c) and (3a)-(3c) depict the trajectories, in the (x, t) -plane, of shock waves (drawn as dashed lines along which $x = \sigma t$) and of characteristics (*i.e.*, solutions of $dx/dt = \lambda(U(x/t))$, drawn as solid curves). The blue and red coloring indicates whether the speed of the characteristic is the smaller or larger eigenvalue, respectively, as explained at the beginning of the next section.

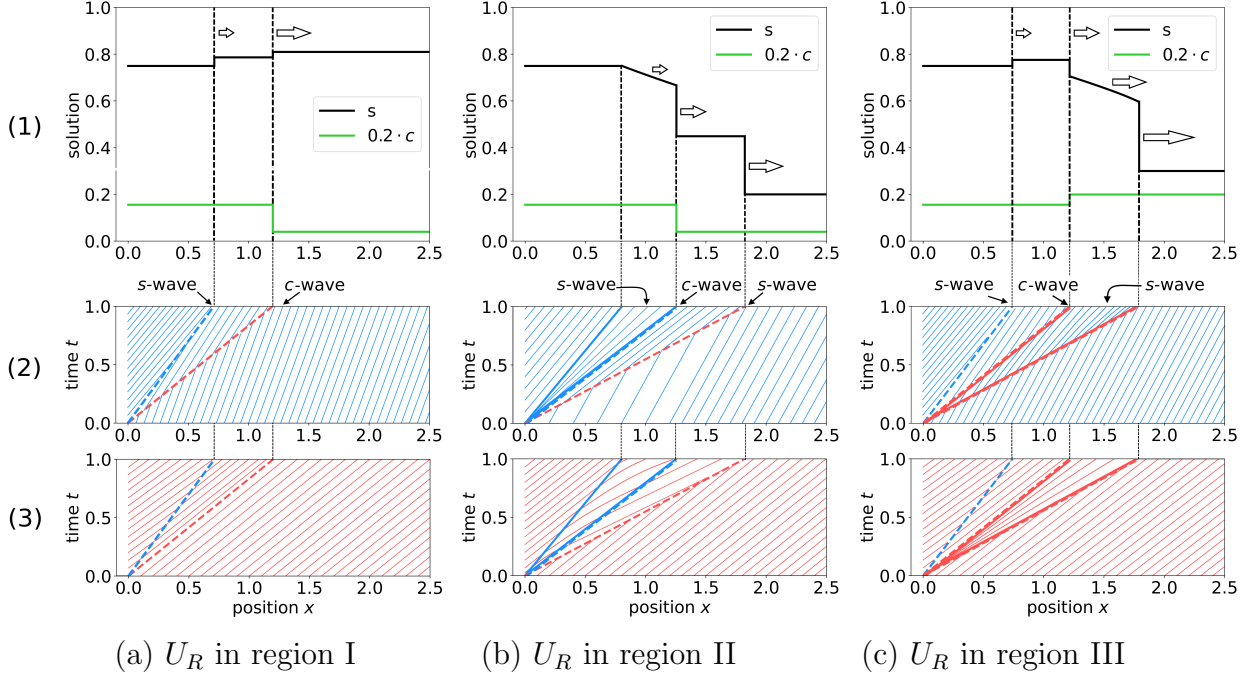


FIGURE 2.4. Examples of three different sequences of waves that are solutions to a Riemann Problem for $U_L \in \{\lambda^s < \lambda^c\}$ and U_R in the respective regions I, II, and III from Fig. 2.2(b).

3. EQUIVALENCE OF ADMISSIBILITY CRITERIA

Recall the standard ordering of the eigenvalues of the characteristic matrix $A(U)$ in (2.6) as $\lambda_1(U) < \lambda_2(U)$, called the 1-family and 2-family characteristic speeds. In polymer models, $\lambda_1(U)$ equals $\lambda^c(U)$ when $U \in \{\lambda^s > \lambda^c\}$, but equals $\lambda^s(U)$ when $U \in \{\lambda^s < \lambda^c\}$.

A standard way to classify a discontinuity is based on the ordering of the characteristic speeds on its two sides relative to its propagation speed σ , *i.e.*, $\lambda_i(U_-) - \sigma$ and $\lambda_i(U_+) - \sigma$

for $i = 1, 2$. See, for example, Refs. [16], [8], and [5, Chapter 8]. Four of the possibilities, which we call the 1-family Lax, 2-family Lax, overcompressive, and crossing configurations of characteristic paths, are depicted in Fig. 3.1:

- 1-family Lax: $\lambda_1(U_-) > \sigma > \lambda_1(U_+)$ along with $\sigma < \lambda_2(U_-)$ and $\sigma < \lambda_2(U_+)$
- 2-family Lax: $\lambda_2(U_-) > \sigma > \lambda_2(U_+)$ along with $\sigma > \lambda_1(U_-)$ and $\sigma > \lambda_1(U_+)$
- overcompressive: $\lambda_1(U_-) > \sigma > \lambda_1(U_+)$ and $\lambda_2(U_-) > \sigma > \lambda_2(U_+)$
- crossing: $\lambda_2(U_-) > \sigma > \lambda_1(U_-)$ and $\lambda_1(U_+) < \sigma < \lambda_2(U_+)$.

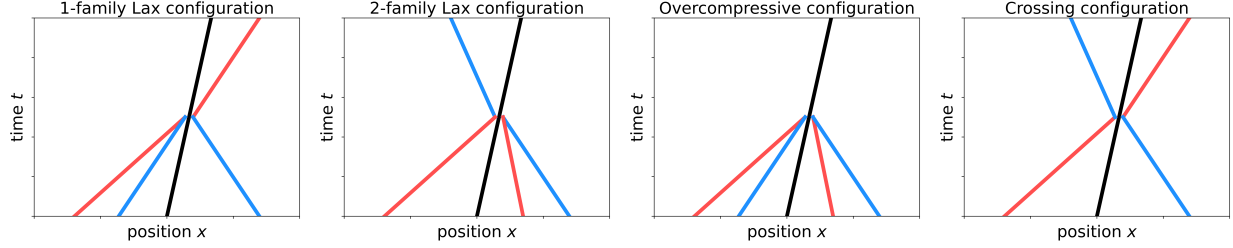


FIGURE 3.1. Four possible configurations of characteristic paths drawn in (x, t) -space: 1-family Lax, 2-family Lax, overcompressive, and crossing. The black line is the shock trajectory with speed σ . Blue curves are characteristic paths for the 1-family, and red curves are for the 2-family.

It will be useful in what follows to extend this classification to contact discontinuities.

Definition 3.1. We adopt the following terminology for configurations of characteristic paths for contact discontinuities, depicted in Fig. 3.2:

- 1-family: $\lambda_1(U_-) = \sigma = \lambda_1(U_+)$ along with $\sigma < \lambda_2(U_-)$ and $\sigma < \lambda_2(U_+)$;
- 2-family: $\lambda_2(U_-) = \sigma = \lambda_2(U_+)$ along with $\sigma > \lambda_1(U_-)$ and $\sigma > \lambda_1(U_+)$;
- overcompressive: $\lambda_1(U_-) = \sigma > \lambda_1(U_+)$ and $\lambda_2(U_-) = \sigma > \lambda_2(U_+)$;
- crossing: $\lambda_2(U_-) > \sigma = \lambda_1(U_-)$ and $\lambda_1(U_+) = \sigma < \lambda_2(U_+)$.

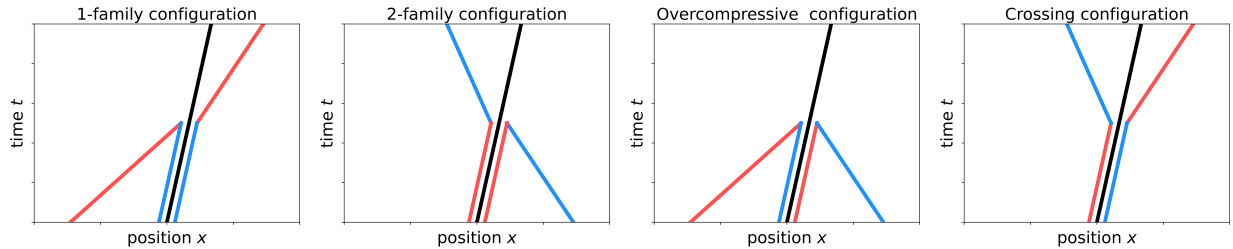


FIGURE 3.2. Four possible configurations of characteristic paths drawn in (x, t) -space for contact discontinuities: 1-family, 2-family, overcompressive, and crossing.

For the polymer model without adsorption, a contact discontinuity with

- 1-family configuration has $U_{\pm} \in \{\lambda^s > \lambda^c\}$;
- 2-family configuration has $U_{\pm} \in \{\lambda^s < \lambda^c\}$;
- overcompressive configuration has $U_- \in \{\lambda^s > \lambda^c\}$ and $U_+ \in \{\lambda^s < \lambda^c\}$;
- crossing configuration has $U_- \in \{\lambda^s < \lambda^c\}$ and $U_+ \in \{\lambda^s > \lambda^c\}$.

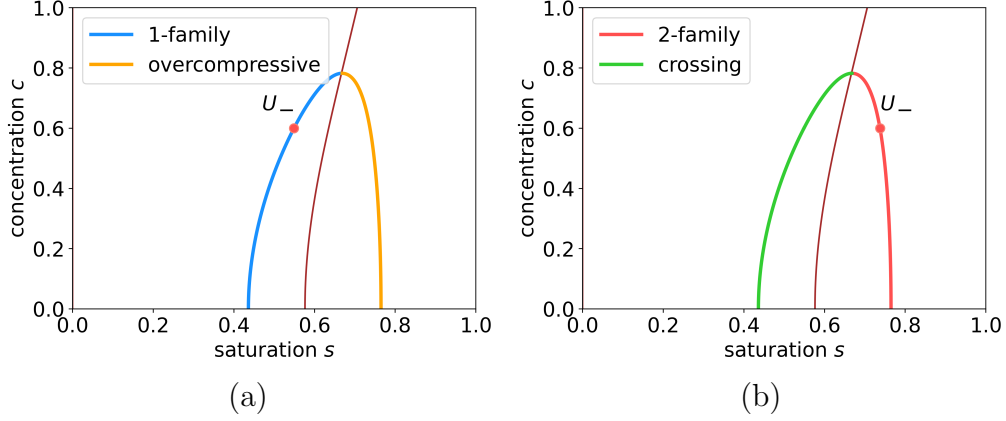


FIGURE 3.3. Contact discontinuities classified according to configuration of characteristics: (a) if $U_- \in \{\lambda^s > \lambda^c\}$, the blue (respectively, orange) curve corresponds to contacts with 1-family (resp., overcompressive) configuration; (b) if $U_- \in \{\lambda^s < \lambda^c\}$, the red (respectively, green) curve corresponds to contacts with 2-family (resp., crossing) configuration.

See Fig. 3.3. Analogous statements are true for each type of c -shock wave in the polymer model with adsorption (1.9).

The main step in proving Theorem 1.5, is the following Lemma 3.2. Theorem 1.5 easily follows from it (for details, see the proof at the end of this section).

Lemma 3.2. *For the polymer model (1.1) that satisfies the monotonicity condition (1.2), contact discontinuities with 1-family, 2-family, and overcompressive configurations of characteristics satisfy the vanishing adsorption admissibility criterion, whereas contact discontinuities with crossing configuration do not.*

Proof of Lemma 3.2. To prove this result, we consider each type of configuration separately. For 1-family, 2-family, and overcompressive configurations we will give explicit sequences of solutions of the system with adsorption (1.9) that tend in L_{loc}^1 to the contact under consideration. For crossing contact discontinuities, we will show that there is no sequence of solutions of Eq. (1.9) that tends in L_{loc}^1 to the contact.

1-family and 2-family contact discontinuities. Let us first prove that 1-family contact discontinuities are admissible under the adsorption criterion. An analogous argument works for the 2-family contact discontinuities. Fix $U_{\pm} = (s_{\pm}, c_{\pm}) \in \{\lambda^s > \lambda^c\}$.

(i) Let $c_- > c_+$, as in Fig. 3.4 (i). Then the contact between U_- and U_+ is the limit of 1-family c -shock waves for the polymer model with adsorption (1.9). Indeed, by Remark 2.2, the c -type branch of the Hugoniot locus $\mathcal{H}_{\alpha}^c(U_-)$ limits to the contact curve $\mathcal{H}_0^c(U_-)$ as $\alpha \rightarrow 0^+$. Consequently, we can choose $U_{\alpha,+} = (s_{\alpha,+}, c_{\alpha,+}) \in \mathcal{H}_{\alpha}^c(U_-) \cap \{\lambda^s > \lambda^c\}$ such that $U_{\alpha,+}$ tends to U_+ as $\alpha \rightarrow 0^+$. Because both U_- and $U_{\alpha,+}$ lie in the region $\{\lambda^s > \lambda^c\}$, a shock wave between U_- and $U_{\alpha,+}$ has the 1-family configuration of characteristics, and thus is admissible for model (1.9). Moreover, by the Rankine-Hugoniot condition (2.5), the speed of this shock wave, σ_{α} , tends to the speed of a contact, σ , as $\alpha \rightarrow 0^+$. From these observations we obtain the convergence of the shock wave between U_- and $U_{\alpha,+}$ to the contact between U_- and U_+ in L_{loc}^1 , so that this contact is admissible by the vanishing adsorption criterion.

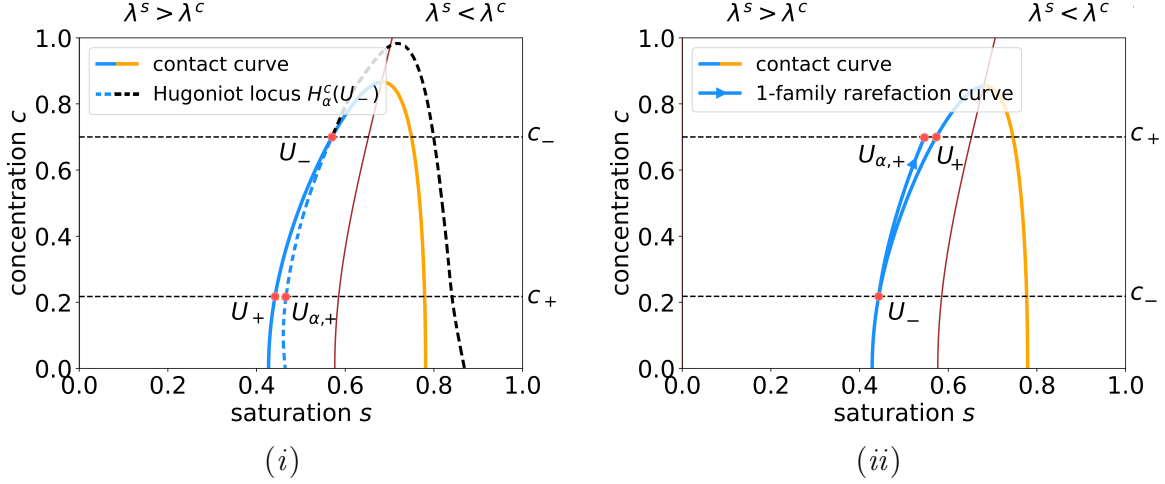


FIGURE 3.4. Schematic illustration for the proof for the 1-family contact discontinuities.

(ii) Let $c_- < c_+$, as in Fig. 3.4 (ii). We can approximate the contact between U_- and U_+ by c -rarefaction waves for the polymer model with adsorption (1.9). Indeed, according to Remark 2.1, for small enough $\alpha > 0$, the c -type integral curve $\mathcal{I}_\alpha(U_-)$ is close to c -type integral curve $\mathcal{I}_0(U_-)$. As a consequence, we can choose $U_{\alpha,+} \in \mathcal{I}_\alpha(U_-) \cap \{\lambda^s > \lambda^c\}$ such that $U_{\alpha,+}$ tends to U_+ as $\alpha \rightarrow 0^+$. Moreover, the characteristic speeds $\lambda_\alpha^c(U_-)$ and $\lambda_\alpha^c(U_{\alpha,+})$ approach each other as $\alpha \rightarrow 0^+$ because of Eq. (2.10):

$$|\lambda_\alpha^c(U_{\alpha,+}) - \lambda_\alpha^c(U_-)| \leq \text{const}_1 \cdot |(D\lambda_\alpha^c) r_\alpha^c| \leq \text{const}_2 \cdot \alpha \rightarrow 0^+,$$

where the constants const_1 and const_2 are independent of α . The characteristic speed $\lambda_\alpha^c(U_-)$ also tends to the contact speed $\sigma = \lambda_0^c(U_-)$ because of Eq. (2.7). We deduce the convergence of the c -rarefaction wave between U_- and $U_{\alpha,+}$ to the contact between U_- and U_+ in L_{loc}^1 , and thus conclude that such a contact is admissible by the vanishing adsorption criterion.

Overcompressive contact discontinuities. Let us prove that overcompressive contact discontinuities are admissible under the vanishing adsorption criterion. Fix $U_- \in \{\lambda^s > \lambda^c\}$ and $U_+ \in \mathcal{H}_0(U_-) \cap \{\lambda^s < \lambda^c\}$. The interesting feature of the overcompressive contact is that it can be represented as a sequence of two shock waves with equal speeds: s -wave between U_- and U_1 , and c -wave between U_1 and U_+ . Here $U_1 = (s_1, c_-) \in \{\lambda^s < \lambda^c\}$ is the uniquely defined state on the contact curve for U_- and the speed of the shocks coincides with the characteristic speed $\lambda_0^c(U_-)$. The properties we assume on f (monotone and S -shape in s , $f(0, c) = f'(0, c) = 0$) guarantee that the s -wave between U_- and U_1 is a shock wave. Notice that the c -wave between U_1 and U_+ is a 2-family contact (see Def. 3.1).

(iii) Let $c_- > c_+$, see Fig. 3.5 (iii). By case (i), the 2-family contact between U_1 and U_+ can be approximated by a sequence of c -shock waves between U_1 and $U_{\alpha,+}$. As a result we get that the sequence of the two waves: s -wave between U_- and U_1 , and c -shock wave between U_1 and $U_{\alpha,+}$ tends in L_{loc}^1 to a contact connecting states U_- and U_+ .

(iv) Let $c_- < c_+$, see Fig. 3.5 (iv). By case (ii), the 2-family contact between U_1 and U_+ can be approximated by a sequence of c -rarefaction waves between U_1 and $U_{\alpha,+}$. As a result we get that the sequence of the two waves: s -wave between U_- and U_1 , and c -rarefaction wave between U_1 and $U_{\alpha,+}$ tends in L_{loc}^1 to a contact connecting states U_- and U_+ .

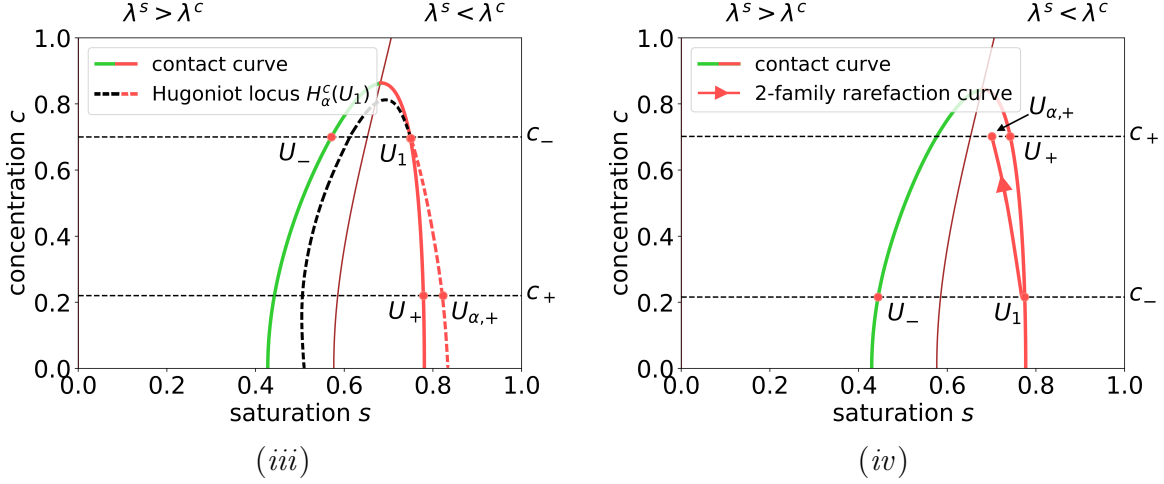


FIGURE 3.5. Schematic illustration for the proof for overcompressive contact discontinuities.

Crossing contact discontinuities. Let us prove that crossing contact discontinuities are not admissible under the vanishing adsorption criterion. Let us fix $U_- \in \{\lambda^s < \lambda^c\}$ along with $U_+ \in \mathcal{H}_0(U_-) \cap \{\lambda^s > \lambda^c\}$.

(v) Assume that $c_- > c_+$, as in Fig. 3.6. (The case $c_- < c_+$ can be proved in a similar fashion.) Let $U_* = (s_*, c_-)$ be the unique point on the interior coincidence locus \mathcal{C}_0 for $c = c_-$. Define

$$\sigma_* := \frac{f(U_*)}{s_*} = f_s(U_*), \quad \delta := |f_s(U_*) - f_s(U_-)| > 0.$$

The proof is by contradiction. Suppose that there exists a sequence of solutions to a Riemann problem for the polymer model (1.9) with left state $U_{\alpha_n,-} = (s_{\alpha_n,-}, c_{\alpha_n,-})$ and right state $U_{\alpha_n,+} = (s_{\alpha_n,+}, c_{\alpha_n,+})$ that tends in L^1_{loc} to a contact that connects states U_- and U_+ as $\alpha_n \rightarrow 0^+$ and $n \in \mathbb{N}$. Then necessarily $U_{\alpha_n,-} \rightarrow U_-$ and $U_{\alpha_n,+} \rightarrow U_+$ as $\alpha_n \rightarrow 0^+$. Fix $\varepsilon \in (0, (c_- - c_+)/2)$; then there exists $\bar{\alpha} > 0$ such that, for all $\alpha_n \in (0, \bar{\alpha})$, the state $U_{\alpha_n,-}$ lies in the ε -neighborhood of U_- and the state $U_{\alpha_n,+}$ lies in the ε -neighborhood of U_+ . We take small enough $\varepsilon > 0$ such that these ε -neighborhoods do not intersect the interior coincidence locus \mathcal{C}_{α_n} if $\alpha_n \in [0, \bar{\alpha})$.

From Sec. 2.2.6 we obtain that any solution to a Riemann problem with left state $U_{\alpha_n,-}$ and right state $U_{\alpha_n,+}$ has the following structure (see Fig. 3.6):

$$U_{\alpha_n,-} \xrightarrow{s} U_{\alpha_n,*} \xrightarrow{c} U_{\alpha_n,**} \xrightarrow{s} U_{\alpha_n,+}.$$

Here $U_{\alpha_n,*} = (s_{\alpha_n,*}, c_{\alpha_n,-})$ is the state on the interior coincidence locus \mathcal{C}_{α_n} for $c = c_{\alpha_n,-}$, and $U_{\alpha_n,**} = (s_{\alpha_n,**}, c_{\alpha_n,+}) \in \{\lambda^s > \lambda^c\}$ is the state on the c -branch of the Hugoniot locus $\mathcal{H}_{\alpha_n}^c(U_{\alpha_n,*})$ for $c = c_{\alpha_n,+}$. Notice that the wave $U_{\alpha_n,-} \xrightarrow{s} U_{\alpha_n,*}$ is an s -rarefaction wave because the flow function $f(s, c_{\alpha_n,-})$ is concave for $s > s_{\alpha_n}$.

To arrive at a contradiction, it is enough to show that the characteristic speeds at the end states $U_{\alpha_n,-}$ and $U_{\alpha_n,*}$ of the s -rarefaction wave do not approach each other as $\alpha_n \rightarrow 0^+$. To this end, notice that the characteristic speed $f_s(U_{\alpha_n,*})$ coincides with the speed of a c -shock

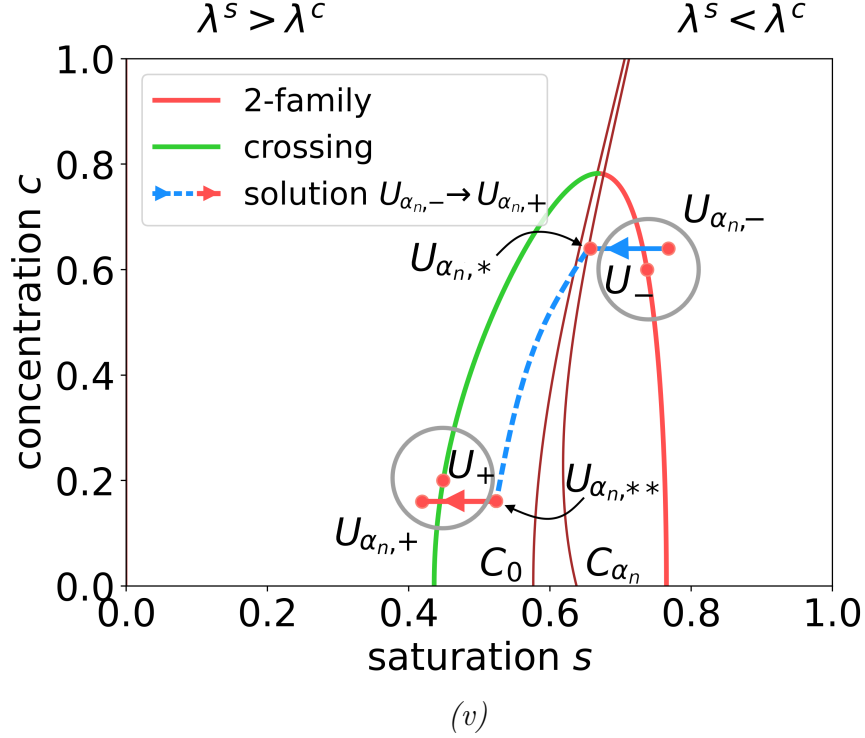


FIGURE 3.6. Schematic illustration for the proof that crossing contact discontinuities are not admissible under the vanishing adsorption criterion.

wave $\sigma_{\alpha_n, *}$:= $\frac{f(U_{\alpha_n, *})}{s_{\alpha_n, *}}$. For α_n small enough we have

$$|f_s(U_{\alpha_n, -}) - f_s(U_-)| < \delta/4 \text{ and } |f_s(U_{\alpha_n, *}) - f_s(U_*)| = |\sigma_{\alpha_n, *} - \sigma_*| < \delta/4.$$

Thus

$$\begin{aligned} |f_s(U_{\alpha_n, -}) - f_s(U_{\alpha_n, *})| &\geq |f_s(U_-) - f_s(U_*)| - |f_s(U_{\alpha_n, -}) - f_s(U_-)| - |f_s(U_{\alpha_n, *}) - f_s(U_*)| \\ &> \delta/2. \end{aligned}$$

The constant δ does not depend on α_n , so we find a contradiction. *Lemma 3.2 is proved.*

To complete the proof of Theorem 1.5, we observe that a contact for which one of the states U_- or U_+ lies on the interior coincidence locus C_0 is also admissible by the vanishing adsorption admissibility criterion.

4. ADSORPTION ADMISSIBILITY OF UNDERCOMPRESSIVE CONTACT DISCONTINUITIES

In Sec. 3, we demonstrated the equivalence of four admissibility criteria for contact discontinuities, summarized in Defs. 1.1–1.4, assuming that the model obeys the monotonicity condition (1.2). We now present an example of a non-monotone model with undercompressive contact discontinuities that are admissible under the de Souza-Marchesin and the adsorption criteria but not under the Keyfitz-Kranzer/Isaacson or Isaacson-Temple criteria. Therefore if the monotonicity condition is violated, these criteria can be distinct.

Consider a chemical flooding model (1.1) with a simple non-monotone flow function, namely the “boomerang” model of Ref. [1]. For each $s \in (0, 1)$, the fractional flow $f(s, c)$

decreases as c ranges from 0 to some value $c^M \in (0, 1)$, and it increases as c ranges from c^M to 1, returning to the same value $f(s, 1) = f(s, 0)$. An example, shown in Fig. 4.1(a), is

$$f(s, c) := \frac{s^2}{s^2 + \mu(c)(1-s)^2} \text{ with } \mu(c) := 1 + 4c(1-c), \quad (4.1)$$

for which $c^M = 0.5$.

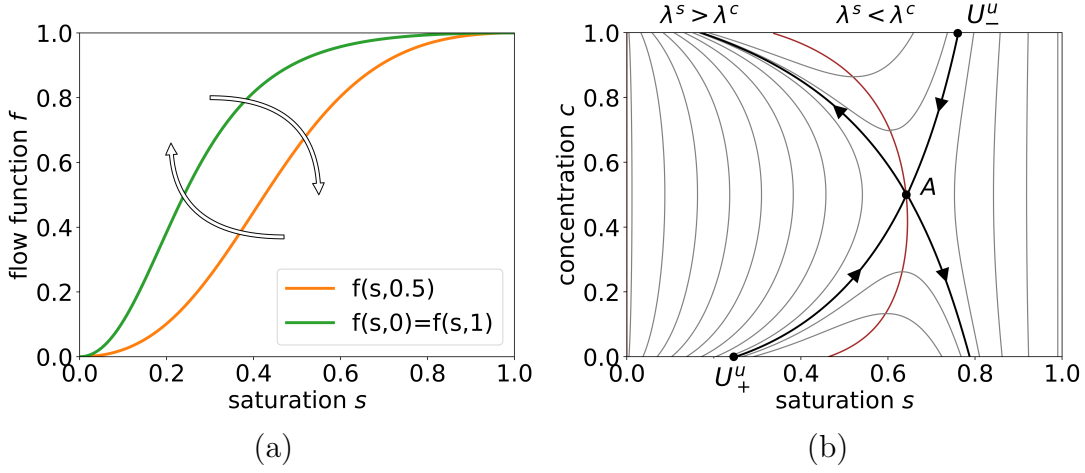


FIGURE 4.1. (a) Fractional flow function $f(s, c)$ defined by formula (4.1). (b) Contact curves for the boomerang model.

The contact curves for system (1.1) are the level sets of the eigenvalue $\lambda_0^c = f/s$; equivalently, they are orbits of the ordinary differential equation $\dot{U} = r_0^c(U)$, where r_0^c is given by Eq. (2.8). This equation has an equilibrium when $f_c = 0$ and $\lambda^s = \lambda_0^c$, such as at the point A on \mathcal{C}_0 where $c = c^M$. The nature of such an equilibrium is determined by the derivative Dr_0^c evaluated at the equilibrium. A straightforward calculation finds that its determinant equals $-(f_{sc})^2 + f_{ss}f_{cc}$. For the boomerang model, this quantity is negative, so that its equilibrium is a saddle-point.

The contact curves for the boomerang model are depicted in Fig. 4.1(b). The structure of solutions to local Riemann problems near this equilibrium was considered by de Souza and Marchesin [6]. The authors proved that there exists an undercompressive contact *i.e.*, a contact with crossing characteristic configuration that is admissible under de Souza-Marchesin admissibility criterion. In this section we want to show that this undercompressive contact is also admissible under the adsorption criterion (Theorem 1.8).

Fix two points in the stable manifold of the equilibrium A ,

$$U_-^u = (s_-^u, 1) \in \{\lambda^s < \lambda^c\} \text{ and } U_+^u = (s_+^u, 0) \in \{\lambda^s > \lambda^c\}, \quad (4.2)$$

as in Fig. 4.1(b). The corresponding speed σ^u can be calculated from the Rankine-Hugoniot condition (2.19). As the contact curve connecting points U_-^u and U_+^u is continuous and monotone in c , it represents contacts that are admissible by the de Souza-Marchesin admissibility criterion; see Def. 1.3. However, it fails to satisfy the Keyfitz-Kranzer/Isaacson and Isaacson-Temple admissibility criteria because U_+^u and U_-^u lie on opposite sides of the interior coincidence locus.

To apply the adsorption criterion, one needs to adopt an admissibility criterion for weak solutions of the system (1.9). We will use the following viscosity criterion of Ref. [1].

Definition 4.1 (Bakharev *et al.* [1]). Fix $\kappa > 0$. We say that a c -shock is admissible if it is the limit of traveling wave solutions of the system

$$\begin{cases} s_t + f(s, c)_x = \varepsilon_c s_{xx}, \\ [cs + \alpha a(c)]_t + [cf(s, c)]_x = \varepsilon_c (cs_x)_x + \varepsilon_d c_{xx} \end{cases} \quad (4.3)$$

as $\varepsilon_c \rightarrow 0^+$ and $\varepsilon_d \rightarrow 0^+$ with fixed ratio $\varepsilon_d/\varepsilon_c =: \kappa$.

Remark 4.1. *If we do not assume $\varepsilon_d/\varepsilon_c$ to be a fixed constant, then, as shown in Ref. [1], there are multiple solutions to some Riemann problems, depending on the value κ . Fixing the value of the parameter κ resolves this problem. Moreover, as one can ascertain from the proof of Theorem 1.8, the precise value of κ does not affect its conclusion.*

Now we are ready to prove Theorem 1.8.

Proof. The main idea of the proof is to show that the undercompressive contact can be approximated by a sequence of undercompressive c -shock waves for the system (1.9) satisfying the viscosity criterion. The existence of undercompressive c -shock waves is shown in Ref. [1]:

Proposition 4.2 (Bakharev *et al.* [1]). *Consider the family conservation laws (1.9), parameterized by $\alpha > 0$, with flux function f defined in Eq. (4.1). There exist functions of $\sigma_{\min}(\alpha)$ and $\sigma_{\max}(\alpha)$ with $0 < \sigma_{\min}(\alpha) < \sigma_{\max}(\alpha) < \infty$ such that for every $\kappa = \varepsilon_d/\varepsilon_c \in (0, +\infty)$, there exist unique functions*

- $s_-^\kappa(\alpha) \in [0, 1]$ and $s_+^\kappa(\alpha) \in [0, 1]$ and
- $\sigma^\kappa(\alpha) \in [\sigma_{\min}(\alpha), \sigma_{\max}(\alpha)]$

such that the undercompressive c -shock wave from $U_-^\kappa(\alpha) := (s_-^\kappa(\alpha), 1)$ to $U_+^\kappa(\alpha) := (s_+^\kappa(\alpha), 0)$ with speed $\sigma^\kappa(\alpha)$ is admissible by the viscosity criterion of Def. 4.1.

Remark 4.2. *Using the results of Ref. [1, Section 4.2.2], one obtains the explicit expressions for $\sigma_{\min}(\alpha)$ and $\sigma_{\max}(\alpha)$; see Fig. 4.2 (a) for the geometric representation. In particular,*

- $\sigma_{\min}(\alpha)$ equals the minimum, with respect to $c \in [0, 1]$, of the slope of the tangent to the graph of $f(\cdot, c)$ that starts at $Q(\alpha) := (-\alpha a_1(1), 0)$. By formula (4.1), this value is obtained for $c = 0.5$, i.e., for the orange curve $f(\cdot, 0.5)$. Notice that

$$\sigma_{\min}(\alpha) \rightarrow \sigma^u \text{ as } \alpha \rightarrow 0^+. \quad (4.4)$$

- $\sigma_{\max}(\alpha)$ equals the slope of the tangent to the graph of $f(\cdot, 0) = f(\cdot, 1)$, drawn in green, that starts at $Q(\alpha)$. As the function $f(\cdot, 0)$ is S -shaped for all α in some interval $[0, \bar{\alpha}]$, we find that

$$\sigma_{\max} := \limsup_{\alpha \in [0, \bar{\alpha}]} \sigma_{\max}(\alpha) < \infty.$$

Let us fix $\kappa > 0$. In what follows we suppress the superscript κ , writing $\sigma(\alpha)$ instead of $\sigma^\kappa(\alpha)$, etc.

To prove Theorem 1.8, it suffices to prove the next Lemma.

Lemma 4.3. $\lim_{\alpha \rightarrow 0^+} \sigma(\alpha) = \sigma^u$, $\lim_{\alpha \rightarrow 0^+} U_-(\alpha) = U_-^u$, and $\lim_{\alpha \rightarrow 0^+} U_+(\alpha) = U_+^u$.

Indeed, Lemma 4.3 implies that the undercompressive c -shock waves connecting states $U_-(\alpha)$ and $U_+(\alpha)$ converge to the undercompressive contact connecting states U_-^u and U_+^u in L_{loc}^1 as $\alpha \rightarrow 0^+$.

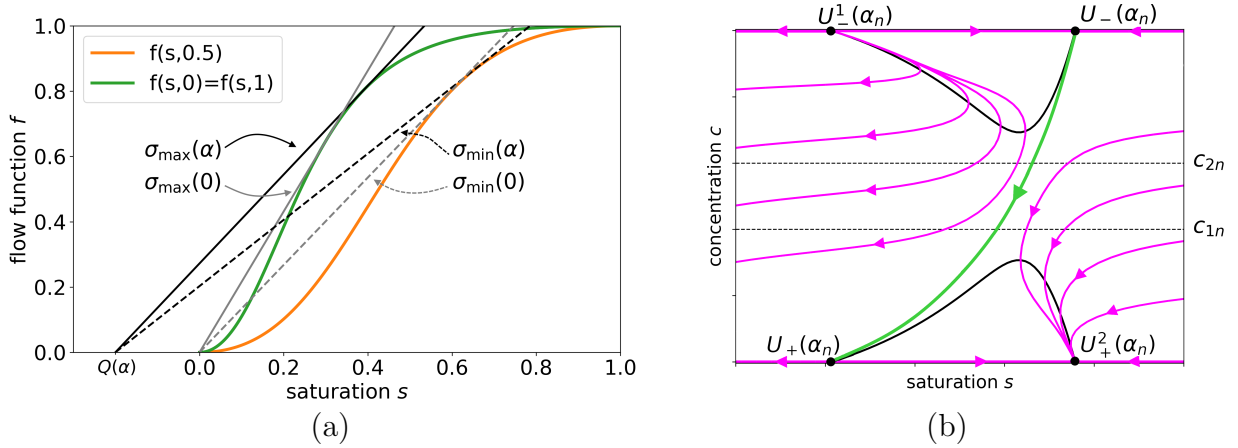


FIGURE 4.2. (a) The geometric determination of $\sigma_{\min}(\alpha)$ and $\sigma_{\max}(\alpha)$ for $\alpha \geq 0$. The green curve is the graph of $f(\cdot, 0) = f(\cdot, 1)$; the orange curve is the graph of $f(\cdot, 0.5)$. (b) Phase portrait for the dynamical system (4.5). The green curve is the heteroclinic orbit joining the two saddle points $U_-(\alpha_n)$ and $U_+(\alpha_n)$, whereas the purple curves are other representative orbits. The black curves are where $s_\xi = 0$.

Proof of Lemma 4.3. First, let us prove that $\sigma(\alpha) \rightarrow \sigma^u$ as $\alpha \rightarrow 0^+$. We will show that $\sigma(\alpha)$ has a unique accumulation point, namely σ^u . Choose a positive sequence $\{\alpha_n\}$ for $n \in \mathbb{N}$ such $\alpha_n \rightarrow 0^+$ and $\sigma_n := \sigma(\alpha_n)$ converges to some limit σ_∞ . By Remark 4.2, we have that $\sigma_\infty \in [\sigma^u, \sigma_{\max}]$.

Let us prove that $\sigma_\infty = \sigma^u$ by contradiction. Assume, to the contrary, that $\sigma_\infty > \sigma^u$. Consider a traveling wave solution of system (4.3) that connects $U_-(\alpha_n)$ and $U_+(\alpha_n)$ (which exists by Proposition 4.2). This solution has the form $s(x, t) := s(\xi)$ and $c(x, t) := c(\xi)$, where $\xi := [x - \sigma(\alpha_n)t]/\varepsilon_c$; it satisfies $s(\pm\infty) = s_\pm(\alpha_n)$, $c(-\infty) = 1$, and $c(+\infty) = 0$. Substituting into (4.3) and simplifying in the standard way (see *e.g.*, [1, Sec. 4.1]), we obtain the following system of ordinary differential equations

$$\begin{cases} s_\xi = f(s, c) - \sigma_n(s + \alpha_n a_1(1)), \\ c_\xi = (\sigma_n \alpha_n / \kappa) [a_1(1)c - a_1(c)]. \end{cases} \quad (4.5)$$

The limit of the system (4.5) as $\alpha_n \rightarrow 0^+$ is the system

$$\begin{cases} s_\xi = f(s, c) - \sigma_\infty s, \\ c_\xi = 0. \end{cases} \quad (4.6)$$

For all $\sigma_n \in (\sigma_{\min}(\alpha_n), \sigma_{\max}(\alpha_n))$, the phase portrait has the structure illustrated in Fig. 4.2(b). (See Ref. [1, Sec. 4.3] for a detailed analysis of properties of trajectories.) In particular, there exists the saddle-to-saddle connection, drawn in green, between the equilibria U_- and U_+ ; it can be parameterized by a function $s = s_{\text{orbit}}(c)$.

Following Ref. [1], we examine the saturation nullcline of this system, *i.e.*, the zero-set of the Eq. (4.5), and its concentration counterpart. The saturation nullcline $\{(s, c) : s_\xi = 0\}$ is drawn as black curves. Because a_1 is concave, the concentration nullcline $\{(s, c) : c_\xi = 0\}$

consists of two lines:

$$\{(s, c) : a_1(1)c - a_1(c) = 0\} = [0, 1] \times \{0\} \cup [0, 1] \times \{1\}.$$

In the terminology of Ref. [1, Sec. 4.2.2], the saturation nullcline of system (4.5) has Type II. In particular, it satisfies the following properties, depicted in Fig. 4.2(b):

- (1) Because $f(\cdot, c)$ is S-shaped for each c , the saturation nullcline contains at most two points for each fixed concentration c . For $c = 1$, there are exactly two critical points, the repeller $U_-^1(\alpha_n)$ and the saddle point $U_-(\alpha_n)$; and for $c = 0$, there are exactly two critical points, the saddle point $U_+(\alpha_n)$ and the attractor $U_+^2(\alpha_n)$.
- (2) Because f_c changes sign at most once for each s (see formula (4.1)), the saturation nullcline contains at most two points for each fixed s .
- (3) Because σ_n belongs to the interval $(\sigma_{\min}(\alpha), \sigma_{\max}(\alpha))$, there exist two sequences in $[0, 1]$, $\{c_{1n}\}$ and $\{c_{2n}\}$ for $n \in \mathbb{N}$, such that no point (s, c) on the saturation nullcline has $c \in [c_{1n}, c_{2n}]$.

The saturation nullcline $\{s_\xi = 0\}$ for the system (4.5) are continuous in α . with respect to α_n as $\alpha_n \rightarrow 0^+$. If $\sigma_\infty = \sigma_T$, then for large enough n the saturation nullcline is close to the set $\{f(s, c) = \sigma^u s\}$, which coincides with the stable and unstable manifolds of the equilibrium A ; see Fig. 4.1(b). This leads to $|c_{2n} - c_{1n}| \rightarrow 0^+$ as $\alpha_n \rightarrow 0^+$. Arguing by contradiction, we assume that $\sigma_\infty > \sigma_T$, which means that the saturation nullcline stays close to the set $\{f(s, c) = \sigma_\infty s\}$, which satisfies the properties (1)-(3). Therefore, there exists an interval $[d_1, d_2] \subseteq (0, 1)$ and $N \in \mathbb{N}$ such that $[d_1, d_2] \subseteq [c_{1n}, c_{2n}]$ for all $n > N$. Thus there is no point (s, c) on the saturation nullcline with $c \in [d_1, d_2]$. It follows that

$$f(s, c) - \sigma_n(s + \alpha_n a_1(1)) < 0 \text{ for all } s \in (0, 1), c \in [d_1, d_2], \text{ and } n > N.$$

Hence for some $\varepsilon > 0$, we have that

$$(\sigma_n \alpha_n)^{-1} \frac{s_\xi}{c_\xi} = \frac{f(s, c) - \sigma_n(s + \alpha_n a_1(1))}{\kappa^{-1}(a_1(1)c - a_1(c))} > \varepsilon > 0 \text{ for all } s \in (0, 1), c \in [d_1, d_2], \text{ and } n > N.$$

Therefore, there exists $\alpha_* = 2 \cdot (\varepsilon \cdot \sigma^u \cdot (d_2 - d_1))^{-1}$ such that for all $\alpha \in (0, \alpha_*)$ and any trajectory $s(c)$ joining the saddle points $U_-(\alpha_n)$ and $U_+(\alpha_n)$,

$$\frac{d}{dc} s(c) > \frac{1}{d_2 - d_1} \text{ for all } c \in [d_1, d_2].$$

Consider the linear function (a barrier)

$$l_1(c) = \frac{c - d_1}{d_2 - d_1}.$$

There is no trajectory, from either U_- or U_+ , that intersects the graph $s = l_1(c)$. Thus the trajectory between saddle points does not exist. This is a contradiction with Prop. 4.2. Thus we conclude that $\sigma(\alpha)$ converges to σ^u as $\alpha \rightarrow 0^+$.

Second, let us prove that $U_-(\alpha) \rightarrow U_-^u$ and $U_+(\alpha) \rightarrow U_+^u$ as $\alpha \rightarrow 0^+$. By the Rankine-Hugoniot condition (2.5) for the shock wave connecting states $U_-(\alpha)$ and $U_+(\alpha)$ with speed $\sigma(\alpha)$, we obtain that

$$\sigma(\alpha) = \frac{f(s_-(\alpha), 1)}{s_-(\alpha) + \alpha a_1(1)} \quad \text{and} \quad \sigma(\alpha) = \frac{f(s_+(\alpha), 0)}{s_+(\alpha) + \alpha a_1(1)}. \quad (4.7)$$

Under the restriction that $U_- \in \{\lambda^s < \lambda^c\}$, the first of these relations defines $s_-(\alpha)$ as a function of σ . Moreover, by the implicit function theorem, this dependence is smooth. We

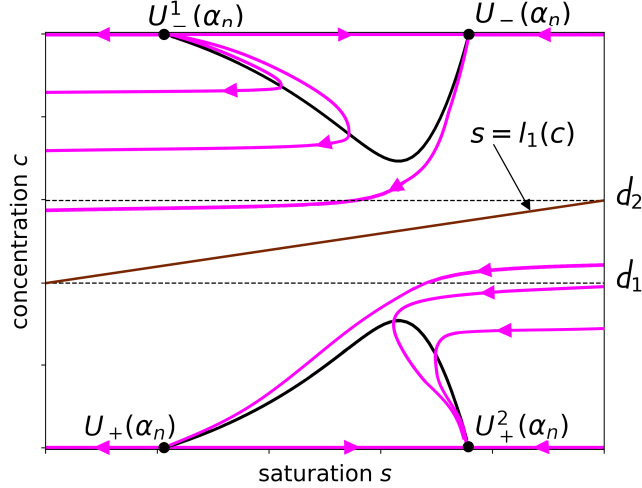


FIGURE 4.3. Illustration of the proof of Lemma 4.3.

know that $\sigma(\alpha)$ tends to σ^u as $\alpha \rightarrow 0^+$; therefore $s_-(\alpha)$ tends to some value s_∞ that satisfies the equation

$$\sigma^u = \frac{f(s_\infty, 1)}{s_\infty} = \lambda_0^c(U_\infty), \text{ where } U_\infty = (s_\infty, 1) \in \{\lambda^s < \lambda^c\}. \quad (4.8)$$

This relation implies that the point U_∞ is located on the stable manifold of the equilibrium A , and due to uniqueness of such a point in the domain $\{\lambda^s < \lambda^c\} \cap \{c = 1\}$, the state U_∞ coincides with the state U_-^u . By analogous reasoning, $U_+(\alpha) \rightarrow U_+^u$ as $\alpha \rightarrow 0^+$. Lemma 4.3 is proved. \square

Let us conclude with two comments. First, although we present an explicit example given by formula (4.1), a similar proof will work for a more general class of Buckley-Leverett functions that change monotonicity in c only once (*e.g.*, the models treated in Ref. [1]).

Second, one can view the adsorption criterion for contact discontinuities from the following perspective. The system for the polymer model (1.1) is a limit of the viscous system (4.3) with adsorption as $\alpha \rightarrow 0^+$, $\varepsilon_c \rightarrow 0^+$, and $\varepsilon_d \rightarrow 0^+$. If we first take the limit as $\alpha \rightarrow 0^+$, we find no traveling wave solutions, hence no solutions satisfying the vanishing viscosity admissibility criterion. Interchanging the limits resolves the issue, at least when the ratio $\varepsilon_d/\varepsilon_c = \kappa$ is held fixed. More precisely, the proof of Theorem 1.8 is valid under the milder condition that $\alpha \cdot \varepsilon_c/\varepsilon_d \rightarrow 0^+$.

5. ACKNOWLEDGMENTS

YP is grateful to Aleksandr Enin for fruitful discussions as well as help with Python scripts for creating figures. YP also thanks IMPA, particularly the Fluid Dynamics Laboratory and Centro PI, for excellent working conditions. DM acknowledges support from FAPERJ: E-26/202.764/2017, CNPq: 306566/2019-2, CNPq: 405366/2021-3, FAPERJ: E-26/201.159/2021. DM is also grateful to Hans Bruining from the Technical University of Delft for sharing his expertise on flow in porous media.

REFERENCES

1. F. Bakharev, A. Enin, Y. Petrova, and N. Rastegaev, *Impact of dissipation ratio on vanishing viscosity solutions of the Riemann problem for chemical flooding model*, arXiv:2111.15001 (2021).
2. P. Bedrikovetsky, *Mathematical theory of oil and gas recovery: with applications to ex-USSR oil and gas fields*, vol. 4, Springer Science & Business Media, 1993.
3. H. Bruining, *Upscaling of single and two-phase flow in reservoir engineering*, Leiden, The Netherlands; CRC Press/Balkema, 2022.
4. S. Buckley and M. Leverett, *Mechanism of fluid displacement in sands*, Transactions of the AIME **146** (1942), no. 01, 107–116.
5. C. M. Dafermos, *Hyperbolic conservation laws in continuum physics*, vol. 3, Springer, 2005.
6. A. J. de Souza and D. Marchesin, *Conservation laws possessing contact characteristic fields with singularities*, Acta Applicandae Mathematica **51** (1998), no. 3, 353–364.
7. E. Hopf, *On the right weak solution of the Cauchy problem for a quasilinear equation of first order*, J. Math. Mech. **19** (1969), 483–487.
8. E. Isaacson, D. Marchesin, and B. Plohr, *Transitional waves for conservation laws*, SIAM journal on Mathematical Analysis **21** (1990), no. 4, 837–866.
9. E. Isaacson, D. Marchesin, B. Plohr, and J. B. Temple, *The Riemann problem near a hyperbolic singularity: the classification of quadratic Riemann problems I*, SIAM J. Appl. Math. **48** (1988), 1009–1032.
10. E. L. Isaacson, *Global solution of a Riemann problem for a non-strictly hyperbolic system of conservation laws arising in enhanced oil recovery*, Rockefeller University, New York, NY, preprint (1981).
11. E. L. Isaacson and J. B. Temple, *Analysis of a singular hyperbolic system of conservation laws*, Journal of Differential Equations **65** (1986), no. 2, 250–268.
12. ———, *Analysis of a singular hyperbolic system of conservation laws*, Journal of Differential Equations **65** (1986), no. 2, 250–268.
13. T. Johansen and R. Winther, *The solution of the Riemann problem for a hyperbolic system of conservation laws modeling polymer flooding*, SIAM journal on Mathematical Analysis **19** (1988), no. 3, 541–566.
14. B. L. Keyfitz and H. C. Kranzer, *A system of non-strictly hyperbolic conservation laws arising in elasticity theory*, Archive for Rational Mechanics and Analysis **72** (1980), no. 3, 219–241.
15. L. Lake, R. Johns, W. R. Rossen, and G. A. Pope, *Fundamentals of enhanced oil recovery*, Society of Petroleum Engineers, Richardson, TX, 2014.
16. P. Lax, *Hyperbolic systems of conservation laws II*, Comm. Pure Appl. Math. **10** (1957), 537–566.
17. O. Oleĭnik, *On the uniqueness of the generalized solution of the Cauchy problem for a non-linear system of equations occurring in mechanics*, Uspehi Mat. Nauk **12** (1957), 169–176.
18. F. Orr, *Theory of gas injection processes*, vol. 5, Tie-Line Publications Copenhagen, 2007.
19. H.-K. Rhee, R. Aris, and N. R. Amundson, *Theory and application of hyperbolic systems of quasilinear equations*, vol. 2, Prentice Hall, 1986.
20. M. Shearer, D. Schaeffer, D. Marchesin, and P. Paes-Leme, *Solution of the Riemann problem for a prototype 2×2 system of non-strictly hyperbolic conservation laws*, Arch. Rational Mech. Anal. **97** (1987), 299–320.
21. J. Smoller, *Shock waves and reaction-diffusion equations*, vol. 258, Springer Science & Business Media, 2012.
22. B. Temple, *Global solution of the Cauchy problem for a class of 2×2 nonstrictly hyperbolic conservation laws*, Advances in Applied Mathematics **3** (1982), no. 3, 335–375.
23. H. Wahanik, *Thermal effects in the injection of CO_2 in deep underground aquifers*, Ph.D. thesis, 2011.

INSTITUTO NACIONAL DE MATEMÁTICA PURA E APLICADA, RIO DE JANEIRO, BRAZIL
 Email address: yulia.petrova@impa.br

LOS ALAMOS, NEW MEXICO, USA
 Email address: bradley.j.plohr@gmail.com

INSTITUTO NACIONAL DE MATEMÁTICA PURA E APLICADA, RIO DE JANEIRO, BRAZIL
 Email address: marchesin@impa.br